Influence of Integrated Optical Feedback on Tunable Lasers

Magnus Happach, David de Felipe, Victor Nicolai Friedhoff, Martin Kresse, Gelani Irmscher, Moritz Kleinert, Crispin Zawadzki, Wolfgang Rehbein, Walter Brinker, Martin Möhrle, Norbert Keil, Werner Hofmann, *Member, IEEE*, and Martin Schell

***Abstract*—In this paper we explain how to use rate equations to describe a laser that includes integrated optical feedback. We find a relation between the threshold current, the voltage drop at the gain section, output power, linewidth, and side mode suppression ratio, and show experimental results.**

***Index Terms*—Gain voltage, continuous tuning, optical feedback, optical feedback interferometry, rate equations, tunable laser, wavelength locking, wavelength stabilization, frequency stabilization, laser stability, side mode suppression ratio, linewidth, output power.**

I. Introduction

OPTICAL feedback interferometry [1]–[3] describes how to use a laser both as a transmitter and a detector at the same time. The laser, acting as a transmitter, emits the beam through an air interface. The beam gets scattered from a device under test and a small part gets reflected back to the laser and is reintroduced into the lasers' cavity. The beam in the cavity interferes with the back reflected beam. The relative phase of the two beams is determined by the phase shift, of the back reflected beam that depends on the change in wavelength and the length of the air interface. Dependent on the phase shift measurable changes occur, e.g. a voltage drop at the gain section [4], from now on refereed as gain voltage, or the output power. Monitoring the parameters enables to determine the displacement [5] or the velocity [6] of the device under test.

The measurement of the gain voltage has also been used to preliminary characterize a laser [7] without optical measurement. The voltage variation has been used to determine the front and back mirror heating powers where the maximum reflection peaks are perfectly aligned. Furthermore, the voltage measurement has been used to actively align the mirrors under operation to grant stable operation [8].

Manuscript received June 27, 2019; revised September 19, 2019; accepted October 7, 2019. Date of publication October 15, 2019; date of current version November 25, 2019. *(Corresponding author: David de Felipe.)*

M. Happach was with the Fraunhofer Heinrich Hertz Institute, 10587 Berlin, Germany. He is now with Sonova AG, 8712 Stäfa, Switzerland.

D. de Felipe, M. Kresse, G. Irmscher, M. Kleinert, C. Zawadzki, W. Rehbein, W. Brinker, M. Möhrle, and N. Keil are with the Fraunhofer Heinrich Hertz Institute, 10587 Berlin, Germany (e-mail: david.felipe@hhi.fraunhofer.de).

V. N. Friedhoff is with the Humboldt University of Berlin, 10117 Berlin (e-mail: nicolai.Friedhoff@mdc-berlin.de).

W. Hofmann is with the Institute for Solid State Physics, Technical University of Berlin, 10623 Berlin, Germany (e-mail: werner.hofmann@tu-berlin.de).

M. Schell is with the Fraunhofer Heinrich Hertz Institute, 10587 Berlin, Germany, and also with the Institute for Solid State Physics, Technical University of Berlin, 10623 Berlin, Germany (e-mail: martin.schell@hhi.fraunhofer.de).

Color versions of one or more of the figures in this article are available online at http://ieeexplore.ieee.org.

Digital Object Identifier 10.1109/JQE.2019.2947560

In order to explain the variations of the parameters of a laser under optical feedback, Lang-Kobayashi [9], [10] set up the rate equations which consider the interference of the cavity beam with the back reflected beam. The photon- and carrier density changes with variation of the strength of the reflectivity, the length of the feedback section and the wavelength. Those parameters have been combined into one effective reflectivity coefficient [11] that reduces the two-cavity problem to a single cavity.

In this paper we propose a model that can be implemented to virtually any tunable laser as long as one can find a reflection point that can be handled as an effective reflectivity. Starting from the model of Lang-Kobayashi, we evaluate expressions for the threshold current, gain voltage, output power, linewidth [12], and side mode suppression ratio [13] (SMSR) of a tunable laser [14], [15] with an active/passive section of the laser cavity. Furthermore, we combine the optical feedback interferometry with the gain voltage measurement at fixed length of the feedback section, which is integrated into the laser chip. This enables to determine the wavelength dependency of a tunable laser under optical feedback. Measuring the voltage fluctuations for a tuned wavelength would help to obtain the absolute distance of a device under test. Variations of the voltage at fixed length of the feedback section could be used to determine wavelength changes which makes the parameter to a monitor signal for active adjustment of the tuning parameters to stably lock the lasers wavelength.

Experimental results are provided based on a tunable InP/polymer DBR laser. We adjusted the tuning parameters to achieve continuous tuning [16] and measured the gain voltage, output power, laser linewidth, and SMSR. Furthermore, we carried out some threshold current measurements by increasing the injection current while simultaneously measuring the output power. Performing this measurement for different phase and Bragg heating powers reveals the threshold current for continuous tuning.

II. Theory

The rate equations from [9] are written with complex amplitudes and with the optical feedback as a delay term. In order to describe the laser analytically, we consider the influence of the optical feedback using the effective mirror model, derived from transmission matrices [13]. The effective reflectivity makes the expression for the mirror losses wavelength dependent and allows a discussion of the rate equations in terms of photon and carrier density.

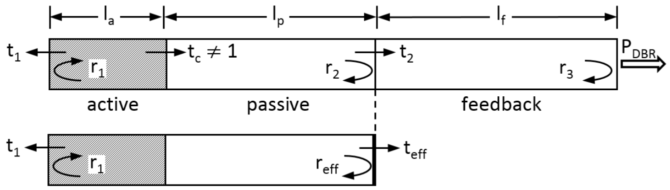

Fig. 1. Laser with active, passive and feedback section in one device with length l_a, l_p and l_f. The left facet with reflection and transmission coefficient r_1, t_1 and the right facet, r_2, t_2 build the laser cavity. The coupling point between passive and active section can be considered with losses and coupling transmission coefficient $t_c \neq 1$. The chip has a feedback section where losses at the coupling point are neglected and ${r_2}^2 + {t_2}^2 = 1$. The output facet has a reflectivity coefficient $r_3 << 1$. The two-cavity setup can be reduced to one cavity by defining the effective reflectivity coefficient r_{eff} at the passive-feedback point with the related effective transmission coefficient t_{eff}.

A. Effective Mirror Model

In order to describe optical feedback by using the effective mirror model we take the theory from [10], [11], [13], [17]. If not mentioned otherwise, all lengths written with a capital L are considered to be the optical length $L = n \cdot l$. with n the refractive index and l the length. Fig 1. shows a laser with an active, passive, and a feedback section with length l_a, l_b, and l_f. The laser cavity is created by the reflection point with reflectivity coefficient r_1 at the left side of the active section and r_2 at the right side of the passive section. The passive and feedback sections are considered ideally coupled with ${r_2}^2 + {t_2}^2 = 1$. The feedback section has a reflection point $r_3 << 1$ and reflects a small part of the emitted laser beam back into the cavity. In order to reduce the two cavities into one, the two reflection coefficients r_2 and r_3 are taken to be an effective reflectivity r_{eff} and can be described by equation (1) [11], [13]. Dependent on the length of the feedback section and the emitted laser wavelength, the reflectivity increases or decreases. Since $r_3 << 1$ and $1 + r_3 \approx 1$, the effective reflectivity can be simplified,

$$\begin{aligned} r_{eff}(\lambda) &= r_2 + \frac{{t_2}^2 r_3 Exp\left[-2i\frac{2\pi}{\lambda}L_f\right]}{1 + r_2 r_3 Exp\left[-2i\frac{2\pi}{\lambda}L_f\right]} \\ &\approx r_2 + {t_2}^2 r_3 Exp\left[-2i\frac{2\pi}{\lambda}L_f\right] \end{aligned} \quad (1)$$

B. Wavelength Dependent Rate Equations

The effective reflectivity changes the mirror loss coefficient $\alpha_m(\lambda)$ dependent on the lasers emitted wavelength and the length of the feedback section. Due to the design of the integrated feedback section, the length L_f can be assumed to be constant. Therefore, some laser parameters become wavelength dependent only and the mirror loss coefficient [13], [18] becomes with the coupling efficiency C_{out} [18] of the active and passive section to

$$\alpha_m(\lambda) = \frac{1}{l_a + l_p} Log\left[\frac{1}{C_{out} r_1 \left|r_{eff}(\lambda)\right|}\right]. \quad (2)$$

Additionally, we can define the average internal loss α of the active and passive section by $\alpha = (\alpha_a l_a + \alpha_p l_p)/(l_a + l_p)$ with the internal losses α_a, α_p of the active and passive sections, respectively. The losses and the average group velocity $v_g = c/n_g$, n_g being the group index and c the velocity of light, impact the photon lifetime λ_{photon}, which is now wavelength dependent due to the wavelength dependent mirror losses. It can be described as

$$\tau_{photon}(\lambda) = [v_g(\alpha + \alpha_m(\lambda))]^{-1}. \quad (3)$$

The fact that the laser beam propagates in the active as well as in the passive section changes the total confinement factor to $\Gamma = \Gamma_{xy} L_a/(L_a + L_p)$ with Γ_{xy} the transverse confinement factor. The material threshold gain g_{th} can be written in terms of the previously mentioned parameters,

$$g_{th}(\lambda) = \left[v_g \Gamma \tau_{photon}(\lambda)\right]^{-1}. \quad (4)$$

Under consideration of the empirical material gain coefficient g_0 and the transparency carrier density n_{tr}, the threshold carrier density n_{th} becomes

$$n_{th}(\lambda) = n_{tr} Exp\left[\frac{g_{th}(\lambda)}{g_0}\right]. \quad (5)$$

For the steady state, the material gain above threshold can be considered as $g(I > I_{th}) = g_{th}$ as well as the carrier density $n_{carrier}(I > I_{th}) = n_{th}$ [11].

The laser rate equations (6) and (7) can be used to determine the threshold current I_{th}, the gain voltage U_g, the output power P_{out} as well as the linewidth Δv, and the SMSR.

$$\frac{dn_{carrier}}{dt} = \frac{\eta_i I}{qV} - \frac{n_{carrier}}{\tau_{carrier}} - v_g g n_{photon} \quad (6)$$

$$\frac{dn_{photon}}{dt} = \Gamma v_g g n_{photon} + \Gamma \beta_{sp} R_{sp} - \frac{n_{photon}}{\tau_{photon}} \quad (7)$$

$n_{carrier}$	=	carrier density that is above threshold equal n_{th}
η_i	=	current injection efficiency
I	=	injection current
q	=	elementary charge
V	=	$l_a h_a w_a/\Gamma_a$ active region volume
Γ_a	=	confinement factor in the active region
$\tau_{carrier}$	=	carrier lifetime
g	=	material gain that is above threshold equal g_{th}
n_{photon}	=	photon density
β_{sp}	=	reciprocal of the number of available modes in the bandwidth of the spontaneous emission.
R_{sp}	=	number of photons spontaneous generated per unit time per unit volume.

The current injection efficiency considers the terminal current that recombines radiatively and non-radiatively with respect to the total injected current [13]. The laser used in this work is supplied with a constant current source at the gain section. The current injection efficiency is therefore considered to be constant.

C. Wavelength Dependent Laser Parameter

The threshold current [11], [19] can be obtained from equation (6) by requiring the laser to be in steady state, $dn_{carrier}/dt = 0$, and no stimulated emission, $n_{photon} = 0$

$$I_{th}(\lambda) = \frac{n_{th}(\lambda) q V}{\eta_i \tau_{carrier}}. \quad (8)$$

The gain voltage $U_g(\lambda)$ depends on the carrier density within the active region, $n_{th}(\lambda)$. With the intrinsic carrier density n_i, the Boltzmann constant k_B, and the temperature T, the voltage $U_g(\lambda)$ becomes [20], [21]

$$U_g(\lambda) = \frac{2k_BT}{q} Log[n_{th}(\lambda)/n_i]. \quad (9)$$

The total output power $P_{out}(\lambda)$ relies on the differential quantum efficiency $\eta_d(\lambda) = (\eta_i\alpha_m(\lambda))/(\alpha + \alpha_m(\lambda))$ which is defined as the number of photons emitted per electron [11]. However, in a laser with two outputs, the delivered power of each facet has to be considered by the relation of their reflection and transmission coefficients [13]. For the fractional power $P_{DBR}(\lambda)$ at the DBR output, we consider the fractional power factor $F_{DBR}(\lambda)| = |t_{eff}(\lambda)|^2/((1-|r_{eff}|^2)+|r_{eff}|r_1^{-1}(1-r_1^2))$. Furthermore, the transmission through effective length l_{eff} of the effective mirror is lossy with a small uniform loss α_{DBR} and becomes $|t_{eff}(\lambda)|^2 = (1-|r_{eff}|^2)Exp[-\alpha_{DBR}l_{eff}]$. With the Planck constant h, the powers are

$$P_{out}(\lambda) = \eta_d(\lambda)\frac{hc}{q\lambda}[I - I_{th}(\lambda)],$$
$$P_{DBR}(\lambda) = F_{DBR}(\lambda)\, P_{out}(\lambda). \quad (10)$$

The output power also depends on the threshold current, which is wavelength dependent as well, but inversely correlated. For a small enough injection current, I, the wavelength dependency of the threshold current dominates and the output power will have maxima at the gain voltage minima. For sufficient large injection currents, the wavelength dependency of the differential quantum efficiency and the fractional power factor dominate and the maxima of the output power are at the maxima of the gain voltage.

Due to the dependency on the output power, and thus on the differential quantum efficiency and the threshold current, the laser linewidth [12] becomes wavelength dependent as well. As a starting point, we calculate the linewidth $\Delta\nu_0(\lambda)$ of a laser with a gain section only but do consider the additional losses from the roundtrip in the passive section by a modified mirror loss $\alpha_m{}^*(\lambda) = l_a{}^{-1}Log[(C_{out}r_1|r_{eff}(\lambda)|Exp[-\alpha_pl_p])^{-1}]$. For a laser with active and passive section, the roundtrip delay from the passive section reduces the linewidth by the square of the chirp reduction factor $F = 1 + v_al_p/v_pl_a$ [22]. With the threshold inversion factor n_{sp}, the group velocity in the active section v_a and the enhancement Henry factor α_H [23] the linewidth $\Delta\nu(\lambda)$ [24] of a laser with active/passive section becomes

$$\Delta\nu_0(\lambda) = \frac{{\upsilon_a}^2\frac{h}{\lambda}n_{sp}\alpha_m^*(\lambda)\left(\alpha_a+\alpha_m^*(\lambda)\right)\left(1+{\alpha_H}^2\right)}{4\pi\, P_{out}(\lambda)\left(\frac{(r_1+|r_{eff}(\lambda)|)(1-r_1|r_{eff}(\lambda)|)}{r_1\left(1-|r_{eff}(\lambda)|^2\right)}\right)}$$
$$\Delta\nu(\lambda) = \Delta\nu_0(\lambda)\frac{1}{F^2} \quad (11)$$

and shows for sufficient small threshold current the same phase as the wavelength dependent gain voltage. The Henry factor varies with the optical feedback conditions [25] but will considered as constant in further calculations.

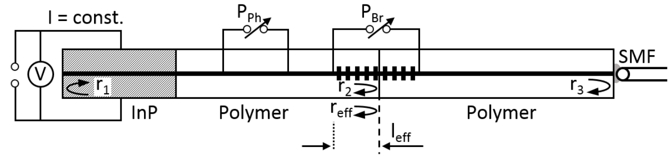

Fig. 2. Tunable Laser with an Indium phosphide (InP) active gain section that is supplied by a constant current source and the voltage measured. The lasers wavelength can be tuned by the phase heating power P_{Ph} and the Bragg heating power P_{Br}. The passive and the feedback section are in the same polymer chip. The chips output is butt-coupled to a single mode fiber (SMF) with phase matching glue.

The SMSR can be written as [13]

$$SMSR_{dB}(\lambda) = 10Log_{10}[\frac{\delta_G(\lambda)+\Delta\alpha(\lambda)+\Delta g(\lambda)}{\delta_G(\lambda)}], \quad (12)$$

where the net modal gain for the main mode is $\delta_G(\lambda_0) = (\alpha + \alpha_m(\lambda_0))\beta_{sp}\eta_rI_{th}(\lambda_0)/(I - I_{th}(\lambda_0))$ with the reciprocal of the number of available modes in the bandwidth of the spontaneous emission β_{sp}, the radiative efficiency η_r, the loss margin $\Delta\alpha = \alpha_m(\lambda_0) - \alpha_m(\lambda_1)$ and the modal gain margin $\Delta g = \Gamma g(\lambda_1) - \Gamma g(\lambda_0)$. The wavelength of the lasing mode is λ_0 and the wavelength of the mode next to it is λ_1. The SMSR should have a minimum for a minimum of the gain voltage because this implies low losses for the lasing mode. However, the shape of the Bragg grating [26] impacts the mirror losses of the lasing mode and its neighbor. As we approximate the maxima surface of the gain distribution and Bragg reflectivity by a normal distribution the theory and the measurement may not show consistent phase dependency.

D. Causal Chain of the Wavelength Dependency

The mirror loss has an impact on the threshold current, the gain voltage, the output power, the linewidth, and the side mode suppression of the laser. The material threshold gain and the threshold carrier density increase with the mirror loss. The increased carrier density increases the threshold current and gain voltage. For a sufficiently large injection current, the output power rises as well. The less optimal laser condition reduces the laser's linewidth and the SMSR decreases. The causality chain can be summarized under the assumption of $I >> I_{th}$ as

$$\alpha_m \uparrow\rightarrow g_{th} \uparrow\rightarrow n_{th} \uparrow\rightarrow I_{th},\quad U_g,\ P_{out} \uparrow\rightarrow \Delta\nu\uparrow,\ SMSR\downarrow \quad (13)$$

III. Experimental Results

In order to test the theory experimentally, we considered a hybrid InP-Polymer laser [15] with a feedback section $L_f = 3388\ \mu m$ and a reflectivity at the output facet like shown in Fig. 2. The lasers cavity consists of the gain section, the phase section, and part of the Bragg section that is considered with an effective length l_{eff} [13]. The facets of the cavity are the gain chips left facet $r_1{}^2 = 0.9$ and the Bragg grating $r_2{}^2 = 0.6$. The excited wavelength of the laser can be tuned by applying heating power at the phase P_{Ph} and the Bragg section P_{Br}. The Laser was tuned continuously as already demonstrated in [27]. The feedback section is located

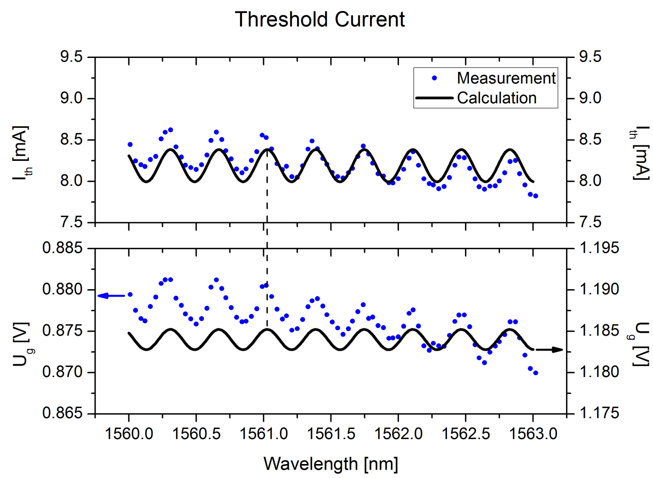

Fig. 3. Measured threshold current and gain voltage (dots) compared to the calculation (solid line).

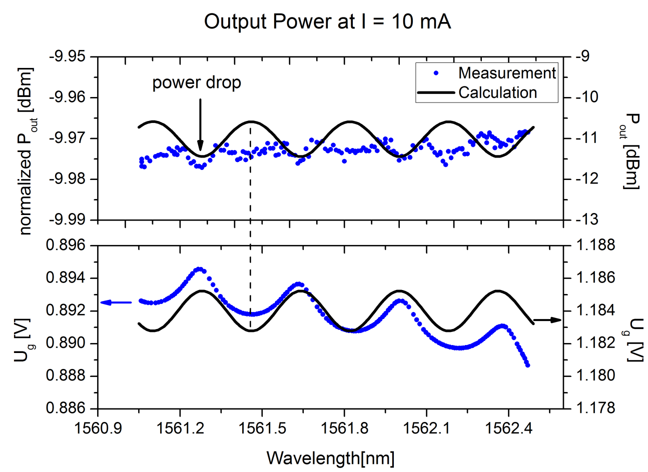

Fig. 4. Measured output Power and gain voltage (dots) compared to the calculation (solid line) of a tunable laser just above threshold. The black arrow marks a power drop. The measured output power has been normalized due to an increased exposure time of the power-meter.

between the right end of the Bragg section and the output facet. The reflectivity r_3 is about −45 dB which stems from a small refractive index change of the butt-coupled polymer to single mode fiber (SMF) coupling point.

Regarding to [1], optical feedback in laser systems can be divided into five different regimes with respect to the feedback power ratio. Due to our laser design, we could exclude our device from regime V and IV because we assume a feedback of at least −10 dB lower. In regime II, the laser would have multiple emission frequencies which can also be excluded from the power spectrum and a SMSR greater than 40 dB. Regime III and I allow single operation with narrowing or broadening linewidth dependent on the phase of the feedback. Our calculations show that the weak feedback of regime I with feedback values lower than −52 dB is not enough to explain the variations of e.g. the voltage. Hence, we assume the laser in regime III with a single emission frequency and dependence on the phase of the feedback.

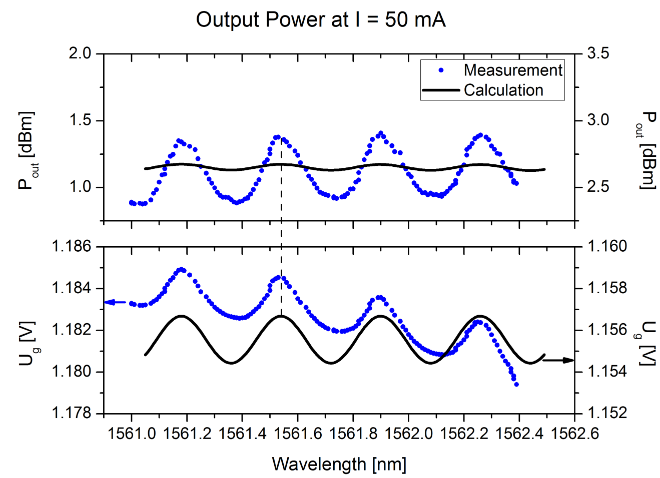

Fig. 5. Measured output Power and gain voltage (dots) compared to the calculation (solid line). For the calculated output power coupling losses between chip and butt-coupled fiber have been considered with 3 dB.

A. Threshold Current

In order to determine the wavelength dependency of the threshold current we performed injection current sweeps for different sets of phase and Bragg heating powers P_{Ph} and P_{Br}. For each sweep the output power was measured. Fitting the power trajectory linearly gives the threshold current [13]. Fig. 3 shows the wavelength dependency of the threshold current I_{th} and the gain voltage U_g. The two parameters show the same wavelength dependency and have the same phase. The solid line shows the theoretical threshold current that was calculated by equation (8) and has its wavelength dependency from the threshold carrier density. The measured and the calculated threshold are in the same range of 8 mA and oscillate with the same amplitude of 0.5 mA. The measured gain voltage is about 310 mV lower compared to the calculation. The measured values oscillate with 5 mV and the calculated values with 2.5 mV.

B. Output Power Just Above Threshold

As shown in Fig. 3, the measured threshold current is about 8.5 mA. In order to support the statement that the output power shows a minimum near the threshold for a maximum of the gain voltage, the laser was tuned continuously with a driving current of I = 10 mA. In order to achieve continuous tuning, the phase- and Bragg heating powers have been applied in such a manner that the wavelength shifts continuously. The exposure time of the power-meter has been increased from 1 ms to 10 ms which normalized the output power by 10 dB. Fig. 4 shows the wavelength dependent gain voltage and normalized output power. The power shows a drop at a maximum of the gain voltage. Regarding equation (10) in this context the injection current I is too small make to the differential quantum efficiency $\eta_d(\lambda)$ the dominating effect. Hence, the losses from the threshold current $I_{th}(\lambda)$ determine the trajectory of the output power and lead to a power drop at a maximum of the gain voltage.

Following the chain of causality from equation (1) to equation (9) we find $r_{eff}(\lambda) \rightarrow \alpha_m(\lambda) \rightarrow \tau_{photon}(\lambda) \rightarrow g_{th}(\lambda) \rightarrow n_{th}(\lambda) \rightarrow U_g(\lambda)$ what shows that the proportionality

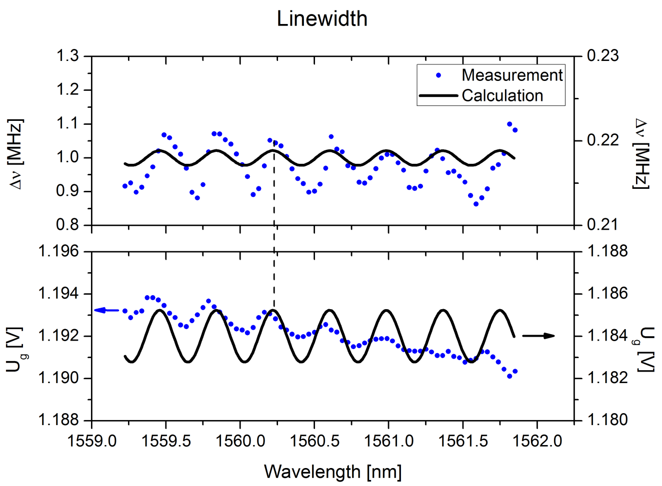

Fig. 6. Measured linewidth and gain voltage (dots) compared to the calculation (solid line).

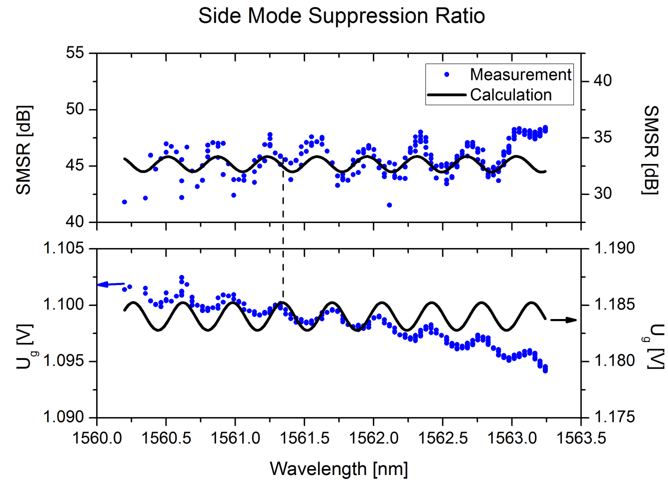

Fig. 7. Measured side mode suppression ratio (SMSR) and gain voltage (dots) compared to the calculation (solid line).

of the gain voltages to the wavelength r_{eff}, is

$$U_g(\lambda) \propto Log[\left|\frac{r_2 r_3 + Exp\left[2i\frac{2\pi}{\lambda}L_f\right]}{r_3 + r_2 Exp\left[2i\frac{2\pi}{\lambda}L_f\right]}\right|] \tag{14}$$

and the peaks became sharper and the valleys broadened.

C. Output Power far Above Threshold

In contrary to the output power just above the threshold, the output power far above threshold shows the same phase and wavelength dependency as the gain voltage. Fig. 5 shows the measured output power and the related gain voltage. The two parameters show the same wavelength dependency and have the same periodicity. The injection current is large enough to compensate its wavelength dependency from the threshold current. Hence, the wavelength dependency of the coupling efficiency is dominating. The calculated output power is about 1.5 dBm higher compared to the measurement. The mismatch might come from higher intrinsic losses or coupling losses between the active/passive section. Coupling losses from the butt-coupling between the chip facet and the single mode fiber has been considered with 3 dB. The amplitude variation shows a mismatch to the theory as well. The measured values vary by 0.5 dBm and the calculated values about 0.04 dBm. In the calculations refractive index changes and frequency shifts, as described by Lang and Kobayashi [9], were not considered and may explain the mismatch. The calculated gain voltage variations are about 2.5 mV and therefore on the scale of the measured values, which are about 2.0 mV. Furthermore, Fig. 5 shows an increasing offset of the voltage to lower wavelengths. Due to the polymers' negative thermo optical coefficient, TO $= -1.1 \cdot 10^{-4} 1/^\circ\text{C}$ [27], heating the Bragg section tunes the grating to a lower wavelength. A higher temperature decreases the refractive index change, lowers the gratings reflectivity and causes a higher mirror loss. As explained in equation (13) an increased mirror loss leads to an increase of the gain voltage.

D. Laser Linewidth

The laser linewidth has been measured for different Bragg and phase heating powers. Fig. 6 shows the wavelength dependent linewidth and gain voltage. The linewidth increases with the voltage as well. The measured linewidth is about 1.0 MHz and oscillates with about 0.2 MHz. The calculated value with 0.218 MHz is one magnitude lower and oscillates with 0.002 MHz. As mentioned in the section above, refractive index changes from the carrier density and frequency changes were not considered and may explain the mismatch.

The wavelength dependency of the linewidth is dominated by the mirror loss $\alpha_{\text{m}}(\lambda)$ and has the same wavelength dependency as the gain voltage. Regarding to equation (11), the output power influences the linewidth in the opposite way than the mirror loss does. However, the impact is too small to change the wavelength dependency compared to the gain voltage.

E. Side Mode Suppression

The side mode suppression ratio and the correlated gain voltage are shown in Fig. 7. The measured SMSR remains over 40 dB and oscillates with an amplitude of 2.5 dB. The calculated SMSR is about 32.5 dB and oscillates with an amplitude of 1.5 dB. The correlated gain voltage shows a maximum at a minimum of the SMSR with a slightly shift.

The SMSR depends on the net modal gain for the main mode, the loss and the modal gain margin. The model gain margin Δg does not have any feedback related wavelength dependency and does not affect the trajectory of the SMSR. The net modal gain $\delta_{\text{G}}(\lambda_0)$ dependents directly on the mirror losses and cause the same wavelength dependency as the gain voltage. Although the loss margin $\Delta\alpha$ is directly influenced by the mirror losses, it has not the same dependency than the gain voltage. Hence, the trajectory of the SMSR depends on the ratio of the reflectivity of the lasing mode with wavelength λ_0 and the mode next to it with wavelength λ_1 and can be expressed as

$$SMSR(\lambda) \propto Log\left[\frac{|r_{eff}(\lambda_0)|}{|r_{eff}(\lambda_1)|}\right]. \tag{15}$$

TABLE I
RATE EQUATION PARAMETER VALUES

Parameter name	Symbol	Value	Unit
Refractive index active medium	n_a	3.4	-
Refractive index passive medium	n_p	1.46	-
Effective group index	ng	3.8	-
Length active medium	l_a	400	µm
Length passive medium	l_p	1500	µm
Effective length of mirror	l_{eff}	500	µm
Width active medium	w	2.1	µm
Height active medium	h	0.04	µm
Coupling efficiency	C_{out}	1	-
Initial gain	g_0	1750	1/m
Transparency carrier density	n_{tr}	$1.57 \cdot 10^{16}$	$1/cm^3$
Waveguide active modal loss	α_a	30	1/cm
Waveguide passive modal loss	α_p	3	1/cm
Reflectivity mirror 1	R_1	0.9	-
Reflectivity mirror 2	R_2	0.6	-
Reflectivity feedback section	R_{fb}	$3 \cdot 10^{-5}$	-
Length of the feedback section	L_{fb}	3388	µm
Threshold inversion factor	n_{sp}	1.5	-
Intrinsic carrier density	N_i	$2.6 \cdot 10^{13}$	$1/cm^3$
Current injection efficiency	η_i	0.85	-
Electron lifetime	τ_e	$1 \cdot 10^{-9}$	s
Confinement factor active region	Γ	0.04	-
Reciprocal of available modes	β	$1.25 \cdot 10^{-5}$	-
Radiative efficiency	η_r	0.8	-
Henry factor	α_H	2.5	-

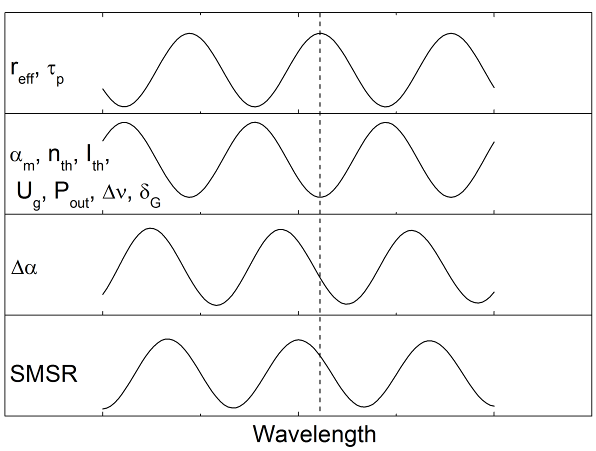

Fig. 8. Wavelength dependency of the effective reflectivity r_{eff}, photon lifetime τ_p, mirror loss α_m, threshold carrier density n_{th}, threshold current I_{th}, voltage at the gain section U_g, output power P_{out}, laser linewidth $\Delta\upsilon$, net modal gain for the main mode δ_G, loss margin $\Delta\alpha$ and side mode suppression ration SMSR of a laser with optical feedback from a reflection point with a constant distance.

IV. CONCLUSION

Starting from the Lang-Kobayashi model, we used the effective reflectivity to set up wavelength dependent equations for the threshold current, gain voltage, output power, linewidth, and side mode suppression ratio. By using a tunable laser, we measured the parameters in dependence on the wavelength and found the experimental data to be agreeable with the theory's predictions. Tracing each parameter with the gain voltage we found that a minimum of the voltage is an excellent indicator for good lasing conditions with reduced linewidth and increased SMSR. A maximum of the voltage indicates maximal output power. Monitoring only the active section, the tuning parameters can be set at an adequate operation point of the laser with regards to output power, SMSR and linewidth. Furthermore, the wavelength dependency of the gain voltage at a fixed, integrated feedback section has been demonstrated.

APPENDIX

Fig. 8 shows the wavelength dependency of different parameters of a laser under optical feedback which comes from a reflection point with a fix distance.

REFERENCES

[1] T. Taimre, M. Nikolić, K. Bertling, Y. L. Lim, T. Bosch, and A. D. Rakić, "Laser feedback interferometry: A tutorial on the self-mixing effect for coherent sensing," *Adv. Opt. Photon.*, vol. 7, no. 3, pp. 570–631, Jun. 2015.

[2] T. M. Bosch, N. Servagent, and S. Donati, "Optical feedback interferometry for sensing application," *Opt. Eng.*, vol. 40, no. 1, pp. 20–28, Jan. 2001.

[3] G. Giuliani, M. Norgia, S. Donati, and T. Bosch, "Laser diode self-mixing technique for sensing applications," *J. Opt. A, Pure Appl. Opt.*, vol. 4, no. 6, pp. S283–S294, Nov. 2002.

[4] Y. L. Lim, J. R. Tucker, and A. D. Rakic, "Distance measurement using the change in junction voltage across a laser diode due to the self-mixing effect," in *Proc. Northern Opt.*, Jun. 2006, pp. 73–77.

[5] C. Bes, G. Plantier, and T. Bosch, "Displacement measurements using a self-mixing laser diode under moderate feedback," *IEEE Trans. Instrum. Meas.*, vol. 55, no. 4, pp. 1101–1105, Aug. 2006.

[6] G. Plantier, N. Servagent, A. Sourice, and T. Bosch, "Real-time parametric estimation of velocity using optical feedback interferometry," *IEEE Trans. Instrum. Meas.*, vol. 50, no. 4, pp. 915–919, Aug. 2001.

[7] G. Sarlet, G. Morthier, and R. Baets, "Control of widely tunable SSG-DBR lasers for dense wavelength division multiplexing," *J. Lightw. Technol.*, vol. 18, no. 8, pp. 1128–1138, Aug. 2000.

[8] G. Sarlet, G. Morthier, and R. Baets, "Wavelength and mode stabilization of widely tunable SG-DBR and SSG-DBR lasers," *IEEE Photon. Technol. Lett.*, vol. 11, no. 11, pp. 1351–1353, Nov. 1999.

[9] R. Lang and K. Kobayashi, "External optical feedback effects on semiconductor injection laser properties," *IEEE J. Quantum Electron.*, vol. QE-16, no. 3, pp. 347–355, Mar. 1980.

[10] K. Peterman, "External optical feedback phenomena in semiconductor lasers," *IEEE J. Sel. Topics Quantum Electron.*, vol. 1, no. 2, pp. 480–489, Jun. 1995.

[11] L. Goldberg, H. F. Taylor, A. Dandridge, J. F. Weller, and R. Miles, "Spectral characteristics of semiconductor lasers with optical feedback," *IEEE Trans. Microw. Theory Techn.*, vol. MTT-30, no. 4, pp. 401–410, Apr. 1982.

[12] C. Herry, "Theory of the linewidth of semiconductor lasers," *IEEE J. Quantum Electron.*, vol. QE-18, no. 2, pp. 259–264, Feb. 1982.

[13] L. Coldren, S. W. Corzine, and M. L. Mashanovitch, *Diode Lasers and Photonic Integrated Circuits*, vol. 218. Hoboken, NJ, USA: Wiley, 2012.

[14] D. de Felipe *et al.*, "40 nm tuneable source for colourless ONUs based on dual hybridly integrated polymer waveguide grating lasers," in *Proc. 39th Eur. Conf. Exhib. Opt. Commun. (ECOC)*, London, U.K., Sep. 2013, pp. 1–3.

[15] D. de Felipe *et al.*, "Polymer-based external cavity lasers: Tuning efficiency, reliability, and polarization diversity," *IEEE Photon. Technol. Lett.*, vol. 26, no. 14, pp. 1391–1394, Jul. 15, 2014.

[16] D. de Felipe *et al.*, "Hybrid polymer/InP dual DBR laser for 1.5 μm continuous-wave terahertz systems," *Proc. SPIE*, vol. 9747, Feb. 2016, Art. no. 974719.

[17] H. Venghaus, *Wavelength Filters in Fibre Optics*, vol. 123. Berlin, Germany: Springer, 2006.

[18] H. Ishii, F. Kano, Y. Yoshikuni, and H. Yasaka, "Mode stabilization method for superstructure-grating DBR lasers," *J. Lightw. Technol.*, vol. 16, no. 3, pp. 433–442, Mar. 1998.

[19] J. Osmundsen and N. Gade, "Influence of optical feedback on laser frequency spectrum and threshold conditions," *IEEE J. Quantum Electron.*, vol. QE-19, no. 3, pp. 465–469, Mar. 1983.

[20] R. Juškaitis, N. P. Rea, and T. Wilson, "Semiconductor laser confocal microscopy," *Appl. Opt.*, vol. 33, no. 4, pp. 578–584, 1994.

[21] J. Katz, S. Margalit, C. Harder, D. Wilt, and A. Yariv, "The intrinsic electrical equivalent circuit of a laser diode," *IEEE J. Quantum Electron.*, vol. QE-17, no. 1, pp. 4–7, Jan. 1981.

[22] R. F. Kazarinov and C. H. Henry, “The relation of line narrowing and chirp reduction resulting from the coupling of a semiconductor laser to passive resonator,” *IEEE J. Quantum Electron.*, vol. QE-23, no. 9, pp. 1401–1409, Sep. 1987.

[23] C. Henry, “Phase noise in semiconductor lasers,” *J. Lightw. Technol.*, vol. 4, no. 3, pp. 298–311, Mar. 1986.

[24] C. Henry, “Theory of spontaneous emission noise in open resonators and its application to lasers and optical amplifiers,” *J. Lightw. Technol.*, vol. 4, no. 3, pp. 288–297, Mar. 1986.

[25] C.-F. Chuang, Y.-H. Liao, C.-H. Lin, S.-Y. Chen, F. Grillot, and F.-Y. Lin, “Linewidth enhancement factor in semiconductor lasers subject to various external optical feedback conditions,” *Opt. Exp.*, vol. 22, no. 5, pp. 5651–5658, 2014.

[26] I. Navruz and A. Altuncu, “Design of a chirped fiber Bragg grating for use in wideband dispersion compensation,” *New Trends Comput. Netw.*, vol. 1, pp. 114–123, Oct. 2005.

[27] M. Happach *et al.*, “Temperature-tolerant wavelength-setting and -stabilization in a polymer-based tunable DBR laser,” *J. Lightw. Technol.*, vol. 35, no. 10, pp. 1797–1802, May 15, 2017.

Magnus Happach received the M.Sc. degree in physics from the Technical University of Berlin in 2015. He was a Student Assistant with the Fraunhofer Heinrich Hertz Institute (HHI) for almost three years. He is currently with Sonova AG, Switzerland.

David de Felipe received the M.Sc. degree in telecommunications engineering from the Universitat Politècnica de València (UPV), Spain, in 2010. He is currently pursuing the Ph.D. degree with the Fraunhofer Heinrich Hertz Institute (HHI) in collaboration with the Technische Universität Berlin (TUB), Germany. His current interests are opto-electronic integrated devices based on a hybrid polymer-InP integration platform, and integrated tunable lasers for telecom, Datacom, and spectroscopy.

Victor Nicolai Friedhoff received the M.Sc. degree in physics from the Humboldt University of Berlin in 2016, where he is currently pursuing the Ph.D. degree in theoretical statistical biophysics. He was a Student Assistant with the Fraunhofer Heinrich Hertz Institute for almost three years while being a student.

Martin Kresse received the master’s degree in physics from TU Berlin. He joined the Fraunhofer Heinrich Hertz Institute (HHI) as a Research Associate in 2018. He is a part of HHI’s Polymer OEIC Group, Photonics Components Department.

Gelani Irmscher received the M.Sc. degree in engineering science from the Technical University of Berlin, Germany, in 2019. He completed the bachelor’s and master’s theses from HHI’s Polymer OEIC Group, Photonics Components Department. He joined HHI’s Polymer OEIC Group, Photonics Components Department, in 2013 as a Student Assistant.

Moritz Kleinert received the master’s degree from TU Berlin and the Ph.D. degree in hybrid photonic integration of graphene-based optoelectronic devices in 2018. He joined the Fraunhofer Heinrich Hertz Institute (HHI) in 2013. He is currently a Project Manager with the Hybrid PICs Group. He has authored or coauthored more than 40 articles in international journals and conference contributions.

Crispin Zawadzki received the Diploma degree in electronic engineering from the Technical University of Berlin in 1995. In 1995, he joined the Fraunhofer Heinrich Hertz Institute. He is currently a Project Leader and has been responsible for the process development and PLC/OEIC-fabrication in several research projects with national and international industrial partners. He has authored or coauthored more than 100 scientific publications and conference papers and holds several patents.

Wolfgang Rehbein joined the Fraunhofer Heinrich Hertz Institute (HHI) in 1987. He is currently with the Photonic Components Department.

Walter Brinker received the Diploma degree in physics from University Münster, Germany, in 1984. In 1985, he joined the Fraunhofer Heinrich Hertz Institute (HHI), Berlin. One focus of his scientific interest is on the optical characterization of III-V-based photonic devices. He is currently involved in the hybrid integration of III-V components with polymeric waveguide structures.

Martin Möhrle received the Ph.D. degree from the Technical University of Berlin in 1992. He has more than 25 years’ of experience and expertise in InP-based lasers, amplifiers, and modulators. He joined the Fraunhofer Heinrich Hertz Institute in 1988. He is currently the Head of the Laser Development Group, Department Photonic Components. He has authored or coauthored of more than 100 articles and holds several patents on laser devices.

Norbert Keil joined the Fraunhofer Heinrich Hertz Institute in 1987. He has more than 30 years of experience in the development of polymer-based hybrid photonic integrated circuits. He is currently the Head of the Hybrid PICs Group and also the Deputy Head of the Photonic Components Department. He has authored or coauthored more than 200 scientific publications and conference papers and holds several patents.

Werner Hofmann (M’06) received the Dipl.-Ing. and Dr.-Ing. degrees from the Technical University of Munich, Germany, in 2003 and 2009, respectively. From 2003 to 2008, he was with the group of Prof. Amann, Walter Schottky Institute, where he was engaged in research on long-wavelength vertical-cavity surface-emitting lasers (VCSELs). Subsequently, he joined the Prof. Chang-Hasnain’s Group, University of California at Berkeley, where he worked on the incorporation of high-contrast gratings into VCSEL devices. In 2010, he joined the Technical University of Berlin as a Principal Scientist with the group of Prof. Bimberg. Since 2013, he has been leading his own group focusing on ultra-high-speed nanophotonic devices. Since 2014, he has also been with Xiamen University, China as a Guest Professor. He is currently a Professor of nanophotonic devices and a CTO of the Center of Nanophotonics, Technical University of Berlin, Germany. He authored more than 100 articles cited more than 500 times and has presented more than ten invited talks and tutorials on international conferences. He is a member of an Association of the German Engineers (VDI), the German Association of University Professors (DHV), and the IEEE Photonics Society.

Martin Schell received the Dipl.-Phys. degree from RWTH Aachen in 1989 and the Dr.rer.nat. degree from the Technical University of Berlin in 1993. He spent one year as a Visiting Researcher with The University of Tokyo, Japan. From 1996 to 2000, he was a Management Consultant with The Boston Consulting Group. From 2000 to 2005, he was a first Product Line Manager and the Head of production and procurement with Infineon Fiber Optics. He is currently a Professor of optic and optoelectronic integration with the Technical University of Berlin, and also the Director of the Fraunhofer Heinrich Hertz Institute. He is a Board Member of the European Photonics Industry Consortium (EPIC) and of OptecBB (Competence Network Optical Technologies Berlin/Brandenburg), and a member of the Photonics21 Board of Stakeholders.